9402 *Biochemistry* **2010,** *49,* 9402–9412
DOI: 10.1021/bi1011546

BIOCHEMISTRY
including biophysical chemistry & molecular biology
Article

SufD and SufC ATPase Activity Are Required for Iron Acquisition during in Vivo Fe-S Cluster Formation on SufB[†]

Avneesh Saini,[‡] Daphne T. Mapolelo,[§] Harsimranjit K. Chahal,[‡] Michael K. Johnson,[§] and F. Wayne Outten*[,‡]

[‡]*Department of Chemistry and Biochemistry, University of South Carolina, Columbia, South Carolina 29208, United States, and* [§]*Department of Chemistry and Center for Metalloenzyme Studies, University of Georgia, Athens, Georgia 30602, United States*

Received July 20, 2010; Revised Manuscript Received September 21, 2010

ABSTRACT: In vivo biogenesis of Fe-S cluster cofactors requires complex biosynthetic machinery to limit release of iron and sulfide, to protect the Fe-S cluster from oxidation, and to target the Fe-S cluster to the correct apoenzyme. The SufABCDSE pathway for Fe-S cluster assembly in *Escherichia coli* accomplishes these tasks under iron starvation and oxidative stress conditions that disrupt Fe-S cluster metabolism. Although SufB, SufC, and SufD are all required for in vivo Suf function, their exact roles are unclear. Here we show that SufB, SufC, and SufD, coexpressed with the SufS-SufE sulfur transfer pair, purify as two distinct complexes ($SufBC_2D$ and $SufB_2C_2$) that contain Fe-S clusters and $FADH_2$. These studies also show that SufC and SufD are required for in vivo Fe-S cluster formation on SufB. Furthermore, while SufD is dispensable for in vivo sulfur transfer, it is absolutely required for in vivo iron acquisition. Finally, we demonstrate for the first time that the ATPase activity of SufC is necessary for in vivo iron acquisition during Fe-S cluster assembly.

Iron−sulfur (Fe-S) clusters are required as cofactors in a wide range of critical cellular pathways. Fe-S metalloproteins carry out diverse reactions including electron transfer and substrate binding and activation. Fe-S cluster biosynthesis requires a complex network of proteins that mobilize sulfur and iron, assemble nascent clusters, and transfer Fe-S clusters to target metalloproteins. In eukaryotes, Fe-S cluster assembly proteins are localized at multiple subcellular locations, while the mitochondria in particular play a central role in regulating Fe-S cluster metabolism (*1*). Prokaryotic organisms often contain multiple Fe-S cluster assembly pathways with overlapping but divergent functions depending on environmental conditions and the specific target Fe-S metalloproteins (*2*).

In vivo biosynthesis of Fe-S clusters is complicated by the potential oxidation of both iron and sulfide building blocks, as well as protein cysteinyl ligands, by oxygen or reactive oxygen species. The *sufABCDSE* operon is required for de novo Fe-S cluster biogenesis under iron starvation and oxidative stress conditions in *Escherichia coli* (*3*−*6*). The SufS cysteine desulfurase and SufE sulfur transfer protein together mobilize sulfur from free cysteine as a protein-bound persulfide (R−S−SH) that ultimately is incorporated into the Fe-S cluster as sulfide during assembly (*7*−*9*). The SufA protein is a member of the A-type Fe-S carrier protein family that transfers Fe-S clusters to target apoenzymes (*10*−*12*). The remaining proteins, SufB, SufC, and SufD, form a stable $SufBC_2D$ complex, but the exact in vivo function of this complex is unknown (*4*, *9*).

Recent in vitro studies have shown that both SufB and the $SufBC_2D$ complex can form a [4Fe-4S] cluster that converts to a [2Fe-2S] cluster upon exposure to oxygen (*7*, *13*). Furthermore, in vitro the $SufBC_2D$ complex can transfer Fe-S clusters to the SufA carrier protein as well as directly to the target apoenzyme aconitase B (*13*, *14*). These in vitro studies suggest that the $SufBC_2D$ complex is a novel type of Fe-S scaffold system distinct from the well-characterized IscU or NifU scaffold proteins. Furthermore, it appears that SufB is the specific Fe-S scaffold protein within the $SufBC_2D$ complex. A key question unanswered by previous studies is the exact role of SufC and SufD in Fe-S cluster assembly. SufC is an ATPase with homology to ATPase subunits of membrane transporters, although the $SufBC_2D$ complex is cytoplasmic (*3*). The basal activity of SufC alone is atypically low, but SufC ATPase activity is enhanced by interacting with SufB or SufD separately or as part of the $SufBC_2D$ complex (*15*, *16*). The role of SufD is unknown, although the C-terminal half of SufD does share significant homology with the same region in SufB (45% sequence similarity over the C-terminal 150 residues for each protein). Despite the fact that SufB alone can easily form Fe-S clusters in vitro, deletion of any of the three components (SufB, SufC, or SufD) abolishes Suf[1] function in vivo (*3*−*6*).

The purpose of the present study is to characterize in vivo Fe-S cluster assembly via the Suf pathway, with a focus on the in vivo role of SufC ATPase activity and the SufD protein during in vivo Fe-S cluster assembly on SufB. To address these questions, we purified a polyhistidine-tagged form of SufB after coexpression with SufCDSE. Using this approach, we have found that SufB, SufC, and SufD form at least two distinct complexes in vivo: $SufBC_2D$ and $SufB_2C_2$. Furthermore, we determined that the absence of SufD or loss of SufC ATPase activity disproportionately diminishes iron content in the SufBCD complexes with only a small effect on sulfide content. These results indicate that

[†]This work was supported by National Institutes of Health Grant GM81706 and a Cottrell Scholar Award from the Research Corporation for Science Advancement (to F.W.O.) and by National Institutes of Health Grant GM62524 (to M.K.J.).

*To whom correspondence should be addressed. Tel: 803-777-8151. Fax: 803-777-9521. E-mail: wayne.outten@chem.sc.edu.

[1]Abbreviations: Isc, iron−sulfur cluster; Suf, sulfur mobilization; ATP, adenosine triphosphate; EPR, electron paramagnetic resonance; FAD, flavin adenine dinucleotide; NADPH, nicotinamide adenine dinucleotide phosphate.

 Published on Web 09/21/2010 © 2010 American Chemical Society

SufD and SufC help to mediate iron acquisition during in vivo Fe-S cluster assembly on SufB.

MATERIALS AND METHODS

Strains and Plasmids. SufS and SufE were amplified by PCR as one DNA fragment using the pGSO164 plasmid (*9*) as a template and primers 5′-GGGAATTCCATATGATTTTTTC-CGTCGACAAAGTGCGGGCCGACTTTCCGGTGC-3′ and 5′-GGGAATTCGGTACCTTAGCTAAGTGCAGCGGCTT-TGGCGCGAATTGCGCGAATCAT-3′. The PCR product was digested with *Nde*I and *Kpn*I and cloned into the corresponding sites of pETDuet-1 (Novagen), generating plasmid pFWO467. SufB, SufBC, and SufBCD were amplified by PCR using the pGSO164 plasmid as a template and the following primers: SufB, 5′-GGGAATTCGAATTCGTCTCGTAATAC-TGAAGCAACTGACGATGTAAAAAC-3′ and 5′-GGGAA-TTCCTGCAGTTATCCGACGCTGTGTTCAAGACTGAT-GGCGAGGAG-3′; SufBC, 5′-GGGAATTCGAATTCGTCT-CGTAATACTGAAGCAACTGACGATGTAAAAAC-3′ and 5′-GGGAATTCCTGCAGTTACTGCTGTTCGGTAAGCCA-GCCATAACCCTGCTC-3′; SufBCD, 5′-GGGAATTCGAA-TTCGTCTCGTAATACTGAAGCAACTGACGATGTAAA-AAC-3′ and 5′-GGGAATTCCTGCAGTCATCTTGCACCTC-CTGGCAGCCGTTGACCGATTCG-3′. PCR products were digested with *Eco*RI and *Pst*I and cloned into the corresponding sites of pFWO467 generating plasmids pFWO468 (His_6-SufB), pFWO469 (His_6-SufBC), and pFWO470 (His_6-SufBCD). The SufC(K40R) mutation was introduced into pGSO164 by site-directed mutagenesis using the QuikChange kit (Stratagene) with primers 5′-CCAAACGGTTCGGGCAGAAGTACCTTATC-GGCAACG-3′ and 5′-CGTTGCCGATAAGGTACTTCTGC-CCGAACCGTTTGG-3′. The pGSO164-SufC(K40R) plasmid was used as template for PCR with the primers described above to amplify SufBCD, followed by digestion of the PCR fragment with *Eco*RI and *Pst*I and ligation into the corresponding sites of pFWO467 to generate pFWO471. The sequences of all plasmid inserts were confirmed by DNA sequencing.

Protein Expression and Purification. Recombinant His_6-SufB, His_6-SufBC, and His_6-SufBCD were coexpressed with SufSE from expression vectors pFWO468, pFWO469, and pFWO470 in *E. coli* strain BL21(DE3). Cultures were grown in LB at 37 °C and induced with 100 μM isopropyl β-D-thiogalactoside (IPTG) when OD_{600} = 0.5−0.6 followed by a shift to 18 °C. LB used for these expression studies was made using ultrapure water and typically contained 9 μM iron. After 18 h of induction at 18 °C, the cells were collected by centrifugation and resuspended in anaerobic buffer containing 50 mM Tris-HCl, pH 7.4, 0.5 M NaCl, 20 mM imidazole, and 1 mM phenylmethanesulfonyl fluoride (PMSF) (Sigma), followed by anaerobic sonication and centrifugation to remove the cell debris. The cleared lysate was loaded onto a Ni^{2+}-NTA column in line with an AKTA Prime FPLC system located completely inside an anaerobic Coy chamber. The column was washed with 5 column volumes of 50 mM Tris-HCl, pH 7.4, 0.5 M NaCl, and 20 mM imidazole. His_6-SufB along with any interacting proteins was eluted with an increasing gradient of 20−500 mM imidazole. His_6-SufB or His_6-$SufB_2C_2$ eluted as a single peak, and those fractions were pooled and concentrated anaerobically. Wild-type His_6-$SufBC_2D$ and His_6-$SufBC_2D$-SufC(K40R) protein complexes eluted as two separate peaks (Supporting Information Figure S1; see Results). Fractions from peak 1 and peak 2 were pooled separately and concentrated anaerobically. The proteins were analyzed by SDS−PAGE. To determine UV−visible extinction coefficients and EPR spin concentrations, as well as iron, sulfide, and flavin ratios, the following protein molecular masses were used: His_6-SufB = 56.4 kDa; His_6-$SufB_2C_2$ = 168.0 kDa; wild-type His_6-$SufBC_2D$ peak 1 = 158.4 kDa; His_6-$SufB_2C_2$ peak 2 = 168.0 kDa; His_6-$SufBC_2D$-SufC(K40R) peak 1 = 158.4 kDa; His_6-$SufB_2C_2$-SufC(K40R) peak 2 = 168.0 kDa.

Chemical Analyses. Iron content of purified proteins was determined colorimetrically using ferrozine as described previously (*17*). The acid-labile sulfide content of purified proteins was determined by a previously reported method (*18*). To determine the type of flavin bound to the various proteins, they were denatured by boiling for 10 min, followed by incubation on ice for 5 min. Precipitated protein was removed by centrifugation at 10000*g* for 10 min. The flavin remaining in the supernatant, which was completely oxidized, was analyzed by thin-layer chromatography on silica gel 60 F254 (Merck) with butan-1-ol/acetic acid/water (12:3:5 v/v) as the solvent system (*19*). FMN (MP Biomedicals) and FAD (Sigma) were run as flavin standards. Flavins were detected by their yellow color and by their fluorescence under UV light. For subsequent quantification of $FADH_2$/FAD bound to proteins, the spectrum of the supernatant was recorded with Beckman Coulter DU 800 spectrophotometer after removal of precipitated protein, and the concentration of FAD released was calculated using the molar extinction coefficient for free FAD at 450 nm (ε = 11300 M^{-1} cm^{-1}) (*20*).

Cysteine Desulfurase Activity Assay. Assays were performed using a previously reported method (*9*). Briefly, reactions were carried out anaerobically at 27 °C in 25 mM Tris-HCl, pH 7.4, and 100 mM NaCl, using 1 μM cysteine desulfurase SufS and 4 μM SufE with or without 4 μM $SufBC_2D$, $SufBC_2D$_K40R mutant, or $(His)_6$-$SufB_2C_2$ complex.

Other Spectroscopic Methods. All samples for spectroscopic investigations were prepared under an argon atmosphere (< 5 ppm O_2) in Vacuum Atmospheres or Coy glove boxes unless otherwise indicated. UV−visible absorption was recorded in sealed anaerobic quartz cuvettes at room temperature using a Beckman or Shimadzu UV-3101 PC scanning spectrophotometer. X-band (~9.6 GHz) EPR spectra were recorded using an ESP-300D spectrometer (Bruker, Billerica, MA) equipped with an ER-4116 dual mode cavity and an ESR 900 flow cryostat (Oxford Instruments, Concord, MA). Spin quantifications were carried out using a 1 mM Cu(EDTA) standard and nonsaturating conditions.

Reactivation of Suf Fe-S Cluster Assembly in Crude Lysates. His_6-SufBCD were coexpressed with SufSE from expression vector pFWO470 in *E. coli* strain BL21(DE3). Cell growth and protein induction were performed as described above. A cell pellet harvested from 2 L of LB was resuspended in 15 mL of buffer and lysed anaerobically as described above. L-Cysteine (2 mM), 2 mM Mg^{2+}-ATP, and/or 2 mM NADPH were added to the cleared lysate. The lysate was incubated anaerobically for 2 h at 20 °C. Following incubation, the lysate was loaded onto a Ni^{2+}-NTA column, and His_6-SufB was purified anaerobically as described above. No exogenous iron source was added, but endogenous iron was typically present at 250 μM in the cleared lysate. After removal of total protein from the crude lysate using a YM3 membrane, approximately 5% of total iron (13 μM) remained in the flow-through, presumably bound to low molecular weight species.

RESULTS

$SufBC_2D$ and $SufB_2C_2$, Coexpressed with SufSE, Purify Bound to $FADH_2$ and a [4Fe-4S] Cluster. Despite the clear evidence that SufB and the $SufBC_2D$ complex can form a [4Fe-4S] cluster in vitro, purification of SufB or $SufBC_2D$ after in vivo expression often results in isolation of protein bound to only low levels of iron and acid-labile sulfide that contains no distinguishable Fe-S cluster (*7*, *9*, *13*). Since SufB and $SufBC_2D$ both form [4Fe-4S] clusters after in vitro reconstitution, these studies have not provided insight into the role of SufC and SufD during in vivo Fe-S cluster assembly. To clarify the in vivo Fe-S cluster status of the $SufBC_2D$ complex and to characterize the function of the SufC and SufD proteins for in vivo Fe-S cluster assembly on SufB, we designed a novel coexpression system based on the pETDuet protein expression vector. The *sufBCD* and *sufSE* gene cassettes were cloned at two separate promoter sites within the vector. Utilizing this vector the *sufBCD* genes can be mutated without altering expression of the *sufSE* genes, which is difficult to accomplish if expressing the entire *sufABCDSE* polycistronic message. The *sufA* gene was omitted from this vector because we reasoned that Fe-S cluster accumulation in the $SufBC_2D$ scaffold might be difficult to capture in the presence of SufA due to cluster transfer from $SufBC_2D$ to the SufA Fe-S cluster carrier protein (*14*). Finally, our novel expression vector incorporates a hexahistidine tag at the N-terminus of SufB to allow for one-step anaerobic purification in order to preserve intact Fe-S clusters on SufB and/or $SufBC_2D$.

The chromosomally encoded Suf system in *E. coli* is usually only induced under oxidative stress and iron starvation conditions (*5*, *21*). However, Suf can substitute for the housekeeping Isc Fe-S cluster assembly pathway even under nonstressed conditions, especially if Suf expression levels are increased above their low basal levels (*22*). While it is possible that there are subtle alterations in Suf mechanism under stressed and nonstressed conditions, these previous results indicate that Suf can function under nonstress conditions to replace the Isc system. Therefore, for the present study we coexpressed the SufBCD and SufSE proteins from the pETDUET vector in LB under aerobic conditions. Future studies will also examine Suf expression specifically under stress growth conditions.

Cells coexpressing SufBCD and SufSE were lysed anaerobically, and $(His)_6$-SufB was purified anaerobically using a Ni^{2+}-NTA column. Using a gradient of imidazole, $(His)_6$-SufB eluted in two peaks from the Ni^{2+}-NTA column (Supporting Information Figure S1A). Peak 1 contained approximately 85% of the total eluted protein. SufC and SufD copurified with $(His)_6$-SufB in peak 1 consistent with previous studies showing tight interactions within the complex (Figure 1) (*9*). Gel filtration analysis of peak 1 showed an apparent molecular mass consistent with a $SufBC_2D$ complex as observed previously (data not shown) (*9*, *13*). Peak 1 was initially colored yellowish green, but the yellow color partially faded as the sample was concentrated using a filter with a 30 kDa MW retention limit. Prior to concentrating $(His)_6$-$SufBC_2D$ peak 1 showed a complex UV−visible absorption spectrum with a broad shoulder at 320 nm and features at 439 and 600 nm (Figure 2A). However, the $(His)_6$-$SufBC_2D$ peak 1 spectrum is distinct from the spectrum of [4Fe-4S] $SufBC_2D$ reconstituted in vitro under anaerobic conditions (compare Figure 2A to Supporting Information Figure S1C). Within 5 min of air exposure, the UV−visible absorption spectrum of $(His)_6$-$SufBC_2D$ peak 1 showed the rapid appearance of strong maxima at 369 and 446 nm, and these maxima saturated with

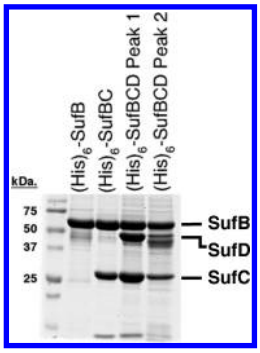

FIGURE 1: SDS−PAGE analysis of proteins and complexes purified using $(His)_6$-SufB expressed from pFWO468, pFWO469, and pFWO470. Samples from each anaerobic purification were separated on a 12% SDS−PAGE gel and stained with Coomassie blue stain.

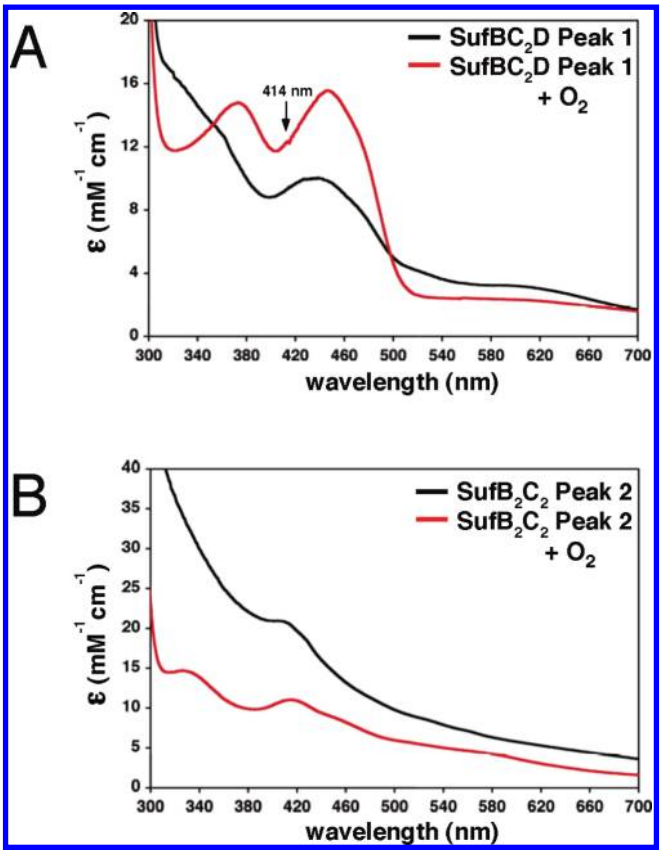

FIGURE 2: Analysis of in vivo purified SufBCD complexes. (A) UV−visible absorption spectra of $(His)_6$-$SufBC_2D$ peak 1 upon initial anaerobic purification (black trace) and after subsequent 10 min exposure to air (red trace). (B) UV−visible absorption spectra of $(His)_6$-$SufB_2C_2$ peak 2 upon initial anaerobic purification (black trace) and after subsequent 10 min exposure to air (red trace). Note that SufS and SufE also were coexpressed with SufBCD in these experiments.

10 min of air exposure (Figure 2A). Absorption maxima at these wavelengths are consistent with the oxidation of a flavin. Simultaneous with the appearance of the 369 and 446 nm maxima during oxygen exposure, the broad shoulder at 320 nm diminishes. The UV−visible absorption spectrum of $(His)_6$-$SufBC_2D$ peak 1 also showed a sharp feature at 414 nm that indicates the presence of an anionic flavin semiquinone species. We confirmed that $(His)_6$-$SufBC_2D$ peak 1 specifically contains $FADH_2$ and not FMN using thin-layer chromatography (data not shown). Quantification of the flavin content of $(His)_6$-$SufBC_2D$ peak 1 indicated the presence of

Table 1: Chemical Analysis of Purified Protein or Complex

protein purified[a]	Fe:protein[b]	S^{2-}:protein[b]	FAD:protein[c]	cluster assembly step[d]
SufB	0.1 ± 0.01	0.9 ± 0.1		
$SufB_2C_2$ subcomplex	0.2 ± 0.08	2.3 ± 0.6	0.8 ± 0.01	2
$SufBC_2D$ peak 1	1.3 ± 0.7	1.8 ± 0.5	1.1 ± 0.04	4
$SufB_2C_2$ peak 2	3.2 ± 0.01	4.2 ± 0.5	0.4 ± 0.05	5
$SufBC_2D$-SufC(K40R) peak 1	0.2 ± 0.04	1.3 ± 0.1	1.0 ± 0.01	3
$SufB_2C_2$-SufC(K40R) peak 2	0.4 ± 0.01	1.1 ± 0.6	0.1 ± 0.03	2

[a]All proteins were purified from cells also coexpressing SufS and SufE (see text for details). See Materials and Methods for molecular masses used to determine ratios of protein to iron and sulfide. [b]Average of triplicate measurements of samples from three independent purifications. [c]Average of two independent purifications (see Materials and Methods for details). [d]Number refers to specific cluster assembly step outlined in Scheme 1. Protein complexes are the products of the indicated step in the assembly cycle. A detailed description of Scheme 1 is provided in the Discussion section.

1.1 $FADH_2$ per $SufBC_2D$ complex immediately after purification (Table 1). During concentration of $(His)_6$-$SufBC_2D$, $FADH_2$ is oxidized to FAD and partially dissociates from $SufBC_2D$ although $SufBC_2D$ still retains about 0.8 $FADH_2$ following concentration. The UV−visible absorption spectrum of the yellow flow-through collected during concentration of $(His)_6$-$SufBC_2D$ peak 1 also showed absorption peaks at 374 and 448 nm although the semiquinone peak at 414 nm was not present in the flow-through (Supporting Information Figure S2A). Recently Wollers et al. also have shown that $SufBC_2D$ reversibly binds $FADH_2$, although the role of the flavin in cluster assembly is still unclear (*13*).

The second peak purified from cells expressing $(His)_6$-SufBCD contained 15% of the total protein isolated. Although peak 2 contained SufB, the ratio of SufC and SufD to SufB was reduced compared to peak 1 (Figure 1). Quantification of the SufB, SufC, and SufD content in both peaks indicated that in peak 2 the SufB:SufC:SufD ratios were 1:1:0.5 while peak 1 showed the previously observed SufB:SufC:SufD ratios of 1:2:1 (Supporting Information Table S1) (*13*). Gel filtration analysis of peak 2 showed one prominent peak, containing SufB and SufC, with an estimated molecular mass consistent with $SufB_2C_2$ stoichiometry and an overall SufB:SufC ratio of 1:1 (data not shown). Thus peak 2 contains a $(His)_6$-$SufB_2C_2$ complex with only residual SufD association. Also apparent in peak 2 were additional proteins not observed in the peak 1 sample. These bands were identified by MS/MS sequencing analysis and found to be SufS and a small amount of partially proteolyzed SufB (Supporting Information Figure S2B).

Peak 2 $(His)_6$-$SufB_2C_2$ was brown, and the UV−visible absorption spectrum (Figure 2B) showed a broad peak at 406 nm that is similar to the spectra of in vitro reconstituted [4Fe-4S] SufB (*7*) or anaerobically reconstituted [4Fe-4S] $SufBC_2D$ (Supporting Information Figure S1C). Upon exposure to air, the $(His)_6$-$SufB_2C_2$ peak 2 UV−visible absorption spectrum (Figure 2B) decreased in overall intensity but showed sharpened peaks at 328 and 416 nm indicating conversion of the [4Fe-4S] cluster to other cluster forms. Interestingly, peak 2 did not show dramatic increases in absorbance at 369 and 446 nm after air exposure. Direct measurement of flavin in peak 2 indicated only 0.4 $FADH_2$ bound per $(His)_6$-$SufB_2C_2$ complex, which was reduced to 0.2 $FADH_2$ per complex after concentration (Table 1).

Peak 1 and peak 2 were retained and concentrated separately under anaerobic conditions. $(His)_6$-$SufBC_2D$ peak 1 contained 1.3 Fe atoms and 1.8 S^{2-} per complex, consistent with the presence of substoichiometric amounts of intact or partially degraded Fe-S clusters (Table 1). The specific type of Fe-S cluster in peak 1 could not be easily characterized by UV−visible spectroscopy due to the presence of strong flavin absorbance features (Figure 2). In contrast, peak 2 $(His)_6$-$SufB_2C_2$ contained 3.2 Fe atoms and 4.2 S^{2-} atoms per complex consistent with the presence of a [4Fe-4S] cluster. Table 1 shows the average iron and acid-labile sulfide content of $(His)_6$-SufBCD peak 1 and peak 2 from triplicate measurements of three independent $(His)_6$-SufBCD purifications. In summary, UV−visible absorption spectroscopy and chemical analysis indicate the isolation of two distinct complexes, $(His)_6$-$SufBC_2D$, with an uncharacterized Fe-S cluster species and stoichiometric $FADH_2$ (peak 1) and $(His)_6$-$SufB_2C_2$ with a [4Fe-4S] cluster and lower amounts of $FADH_2$ (peak 2). The requirement for all three proteins for 1 equiv of flavin binding mirrors the recent results of Wollers et al. (*13*).

To characterize the $FADH_2$ and Fe-S species present in peaks 1 and 2, we conducted a large-scale purification of $(His)_6$-SufBCD under anaerobic conditions in order to prepare a sample that was sufficiently concentrated for subsequent spectroscopic analysis. Initially, we utilized the same linear imidazole gradient for large-scale purification of $(His)_6$-SufBCD that was used for the small-scale preparation. We observed elution of peak 1 and peak 2 similar to that from the small-scale preparations described above (data not shown). However, the run time required to maintain the proper gradient and flow rate was greater for the large column (utilized for the large-scale preparation) than for the small-scale preparation column. During the longer elution phase the Fe-S cluster content of $(His)_6$-$SufB_2C_2$ peak 2 greatly diminished such that it was nearly undetectable after elution and concentration. To avoid this technical problem, we eluted the complexes from a large-scale preparation with a fast step gradient rather than the slow linear gradient. This modified purification protocol allowed us to prepare a concentrated sample containing both $(His)_6$-$SufBC_2D$ and $(His)_6$-$SufB_2C_2$ mixed together in the same elution fractions. The peak 1/peak 2 mixture was frozen in liquid nitrogen either before or after addition of dithionite, and both samples were analyzed by EPR spectroscopy (Figure 3).

The EPR spectra of the purified mixture of $(His)_6$-$SufBC_2D$ and $(His)_6$-$SufB_2C_2$ before and after dithionite reduction provides a preliminary assessment of the nature of the Fe-S clusters. As purified, the EPR spectrum is dominated by a $g = 4.3$ resonance that is generally characteristic of adventitiously bound high-spin ($S = {}^5/_2$) Fe(III) species (Figure 3A). However, in this case, the breadth of the low-field component of the EPR spectrum centered at $g = 9.0$ suggests an alternative assignment. Based on spectroscopic studies of structurally synthetic complexes and "purple" aconitase, the features are characteristic of linear $[3Fe\text{-}4S]^+$ clusters, which also exhibit rhombic $S = {}^5/_2$ ground states (*23*, *24*). Confirmation and quantification of linear $[3Fe\text{-}4S]^+$ clusters in as-purified SufBCD will require detailed Mössbauer and/or variable-temperature MCD studies. It is possible that this linear $[3Fe\text{-}4S]^+$ cluster is an

oxidative degradation product of a [4Fe-4S] cluster (as is the case in aconitase). If so, the degradation pathway for the [4Fe-4S] cluster on the SufB scaffold is distinct from that of the [4Fe-4S] cluster on the IscU scaffold which degrades directly to the [2Fe-2S] form with the concomitant loss of iron and sulfide without forming a stable linear $[3Fe\text{-}4S]^{+}$ intermediate (*25*). This preliminary result is intriguing as both synthetic and biological linear $[3Fe\text{-}4S]^{+}$ clusters have been shown to convert to $[4Fe\text{-}4S]^{2+,+}$ clusters under reducing conditions in the presence of Fe(II) ion (*23*, *26*). Hence it is possible that linear $[3Fe\text{-}4S]^{+}$ clusters are in vivo precursors of [4Fe-4S] clusters on SufB, and experiments are in progress to test this hypothesis

The $g = 2.0$ region of the EPR spectrum of as-purified SufBCD is dominated by an isotopic organic radical resonance centered near $g = 2.01$ (Figure 3A), that is readily observable without broadening at 100 K. This resonance accounts for <0.03 spin/SufBCD complex in as-purified samples, increases to 0.10 ± 0.02 spin/SufBCD complex in samples reduced with stoichiometric dithionite, and is lost in samples reduced with a 10-fold excess of dithionite. The EPR and redox properties are both indicative of a flavin semiquinone as initially suggested by the UV−visible absorption data discussed above and as recently reported for $SufBC_2D$ bound to $FADH_2$ (*13*).

Reduction with a 10-fold excess of dithionite also results in loss of the $g = 9.0$ and 4.3 features of the $S = {}^5/_2$ resonance and the appearance of a near-axial $S = {}^1/_2$ resonance, $g = 2.046$, 1.936, and 1.895, with relaxation properties that are characteristic of a $S = {}^1/_2$ $[4Fe\text{-}4S]^{+}$ cluster (Figure 3B) (i.e., observable without broadening only below 30 K). The resonance accounts for 0.10 ± 0.03 spin/SufBCD complex and is very similar to that reported for $S = {}^1/_2$ $[4Fe\text{-}4S]^{+}$ clusters in dithionite-reduced reconstituted samples of SufB, $g_{||} = 2.042$ and $g_{\perp} \sim 1.93$ (*7*) and to the EPR spectrum of in vitro reconstituted $[4Fe\text{-}4S]^{+}$ $SufBC_2D$ (Supporting Information Figure S3). The low-spin quantification of the as-purified sample is likely to be a consequence of having both conformations (peaks 1 and 2) of SufBCD present in the EPR sample. While only the $SufB_2C_2$ peak 2 appears to contain $[4Fe\text{-}4S]^{2+,+}$ clusters as-purified (based on the UV−visible absorption data in Figure 2B and the iron and sulfide measurements in Table 1), $SufB_2C_2$ only represents about 15% of the total SufBCD protein in the sample (with the remainder being $SufBC_2D$ peak 1). Although we have been unable to observe low-field components indicative of a high-spin ($S > {}^1/_2$) $[4Fe\text{-}4S]^{+}$ cluster in the EPR spectra, we cannot rule out the possibility that the low-spin quantification is also a consequence of a spin state mixture involving a heterogeneous high-spin $[4Fe\text{-}4S]^{+}$ cluster. In summary, the EPR spectroscopy confirms the presence of $[4Fe\text{-}4S]^{2+,+}$ clusters on as-purified $SufB_2C_2$ and suggests that either $SufB_2C_2$ or $SufBC_2D$ may contain linear [3Fe-4S] clusters that have not been previously observed in Fe-S cluster assembly systems such as Isc or Nif.

Although we were able to isolate the $(His)_6$-$SufB_2C_2$ complex bound to [4Fe-4S] clusters, it is possible that formation of this novel complex is an artifact of our protein expression system. A detailed biochemical comparison of $SufBC_2D$ and $SufB_2C_2$ is currently underway. However, in order to test if the $(His)_6$-$SufB_2C_2$ described here has biochemical activity consistent with Fe-S cluster assembly, we determined if as-purified $(His)_6$-$SufB_2C_2$ is able to further enhance the cysteine desulfurase activity of SufS in the presence of SufE as has been previously reported for $SufBC_2D$ (*7*, *9*). The as-purified $(His)_6$-$SufB_2C_2$ complex enhances the activity of SufSE to a similar level as the $SufBC_2D$ complex (Table 2), suggesting that it is a physiologically active complex rather than a purification artifact.

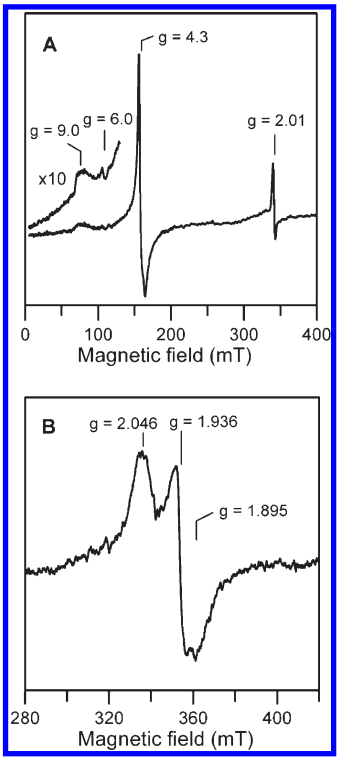

FIGURE 3: EPR spectra of a mixture of purified $(His)_6$-$SufBC_2D$ and $(His)_6$-$SufB_2C_2$ before (A) and after (B) anaerobic reduction with a 10-fold excess of sodium dithionite. Samples contained 0.20 mM $(His)_6$-SufBCD. EPR conditions: temperature, 5.6 K (A) and 10.6 K (B); microwave power, 4 mW (A) and 10 mW (B); modulation amplitude, 0.65 mT (A and B); microwave frequency, 9.5948 GHz (A) and 9.5939 (B). The $g = 6.0$ component in spectrum A results from a minor high-spin ferric heme impurity.

SufC and SufD Are Required for in Vivo Fe-S Cluster Assembly on SufB. To establish the potential role of SufC and/or SufD during Fe-S cluster formation in vivo, we repeated the $(His)_6$-SufB purification from expression vectors for which either SufD or both SufC and SufD were deleted. This allowed us to purify the SufBC subcomplex or SufB alone. Even in the absence of SufD, SufB and SufC can still form a stable complex such that SufC copurifies with $(His)_6$-SufB as a single peak (Figure 1 and data not shown). Similar results were also reported when coexpressing SufB and SufC with a C-terminal polyhistidine tag (*16*). The gel filtration elution profile showed one prominent species that eluted at a molecular mass consistent with a $(His)_6$-$SufB_2C_2$ complex and that was similar to gel filtration elution profile of peak 2 above (data not shown). The UV−visible absorption spectrum of $(His)_6$-$SufB_2C_2$ prior to concentration (Figure 4) revealed the presence of FAD with maxima at 368 and 446 nm similar to that observed for the air-oxidized $(His)_6$-$SufBC_2D$ peak 1 (Figure 2A), indicating that $(His)_6$-$SufB_2C_2$ purifies with $FADH_2$ already partially oxidized to FAD. The flavin content of the $(His)_6$-$SufB_2C_2$ subcomplex was 0.8 FAD per complex, which is double that of $(His)_6$-$SufB_2C_2$ peak 2 (Table 1). In contrast to $(His)_6$-$SufB_2C_2$ peak 2, the $(His)_6$-$SufB_2C_2$ subcomplex expressed without SufD did not show any features indicative of Fe-S clusters, either before or after concentration. After concentration under anaerobic conditions, $(His)_6$-$SufB_2C_2$ contained 0.2 Fe atom and 2.3 S^{2-} atoms per subcomplex (Table 1). For clarity we will hereafter refer to this complex (purified in the absence of SufD expression) as the $(His)_6$-$SufB_2C_2$ subcomplex to differentiate it from the $SufB_2C_2$ peak 2 complex described above (purified after coexpression with SufD).

Table 2: Enhancement of SufS Cysteine Desulfurase Activity

proteins[a]	SufS specific activity[b]
SufS	6.6 ± 0.2
SufS + SufE	31.6 ± 0.4
SufS + SufE + $SufBC_2D$	79.5 ± 5.1
SufS + SufE + $SufB_2C_2$	59.5 ± 2.2
SufS + SufE + $SufBC_2D$-SufC(K40R)	81.2 ± 5.2

[a]SufS was present at 1 μM in all samples. SufE and SufBC(D) complexes were added at 4 μM. [b]Specific activity is nmol of S^{2-} min^{-1} (mg of SufS)$^{-1}$. The average of triplicate measurements is shown.

$(His)_6$-SufB expressed without SufC and SufD also eluted in a single peak. The UV−visible absorption spectrum of SufB showed weak but observable features including a broad shoulder at 320 nm and a broad absorption maxima at 413 nm (Figure 4). After concentration, SufB only contained 0.1 Fe atom and 0.9 S^{2-} atom per monomer (Table 1), indicating negligible amounts of Fe-S cluster. SufB expressed without SufC and SufD did not contain any observable $FADH_2$ or FAD.

The purification studies demonstrate that, though SufB alone can be easily reconstituted with an Fe-S cluster in vitro, deletion of either SufD or both SufC and SufD results in significant reduction of the SufB Fe-S cluster in vivo. These results also indicate that the $SufB_2C_2$ subcomplex can bind $FADH_2$/FAD in vivo while SufB alone does not bind flavin in vivo. A detailed comparison of the $(His)_6$-SufB, $(His)_6$-$SufB_2C_2$, $(His)_6$-$SufBC_2D$ peak 1, and $(His)_6$-$SufB_2C_2$ peak 2 samples shows that the Fe: protein ratios of $(His)_6$-SufB and the $(His)_6$-$SufB_2C_2$ subcomplex were 6−13-fold lower than peak 1 of the $(His)_6$-$SufBC_2D$ complex and 16−32-fold lower than $(His)_6$-$SufB_2C_2$ peak 2 complex (Table 1). In contrast, the S^{2-}:protein ratio of the $(His)_6$-$SufB_2C_2$ subcomplex was approximately the same as $(His)_6$-$SufBC_2D$ peak 1 and only 50% lower than $(His)_6$-$SufB_2C_2$ peak 2 (Table 1). The differential depletion of iron (but not sulfide) in the $(His)_6$-$SufB_2C_2$ subcomplex indicates that SufD is likely required for in vivo iron acquisition during Fe-S cluster assembly on SufB. This is the first reported biochemical requirement for SufD in any step of Suf-mediated Fe-S cluster assembly.

Furthermore, the $(His)_6$-$SufB_2C_2$ subcomplex and the $(His)_6$-$SufB_2C_2$ peak 2 are qualitatively different. While the $(His)_6$-$SufB_2C_2$ subcomplex expressed in the absence of SufD contained no detectable Fe-S cluster, the $(His)_6$-$SufB_2C_2$ peak 2 complex, coexpressed with SufD, appears to contain a [4Fe-4S] cluster (Table 1, Figure 2B, and Figure 3B). This difference indicates that SufD is absolutely required in vivo for efficient Fe-S cluster assembly on SufB. Interestingly, SufD appears to dissociate from SufBC at some point during or after assembly of the [4Fe-4S] cluster and is replaced by a second SufB monomer. At present we cannot determine if SufD dissociates on its own (to be replaced by a single SufB) or as part of a SufCD subcomplex (to be replaced by a SufBC subcomplex). Previous reports have clearly shown that $SufC_2D_2$ can form an independent complex that is stable enough for structural characterization (*16*, *27*). Our present purification strategy utilizing $(His)_6$-SufB would not be able to capture an independent SufCD subcomplex and does not directly address this mechanistic question. However, these results provide the first indication of a separate role for $SufB_2C_2$ after complete cluster assembly.

Characterizing the Role of SufC ATPase Activity for Fe-S Cluster Assembly. Previous studies have shown that SufC is required in vitro for $SufBC_2D$ enhancement of SufS cysteine desulfurase activity and for SufE-SufB interactions during sulfur transfer (*7*). Part of SufC's role in these processes may be to stabilize SufB and/or induce conformational changes in SufB to improve its interaction with SufSE or SufA. To evaluate the role of SufC ATPase activity in vivo without disrupting the integrity of the $SufBC_2D$ or $SufB_2C_2$ complexes, the conserved lysine at position 40 in the Walker A motif of the SufC ATPase was substituted by an arginine within the SufBCD expression plasmid to generate SufC(K40R). Based on the analogous mutation in the MalK ATPase, the SufC K40R mutation allows ATP binding but blocks ATP hydrolysis, thereby locking SufC into the ATP-bound form (*28*). ATPase assays were performed to confirm that the purified $SufBC_2D$-SufC(K40R) complex lacks ATPase activity (data not shown).

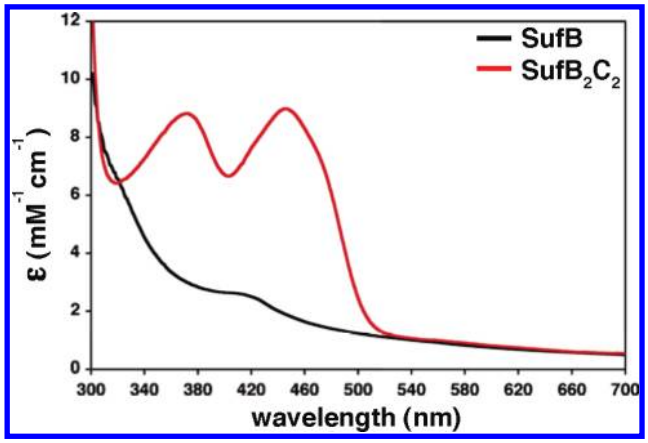

FIGURE 4: UV−visible absorption spectra of $(His)_6$-SufB (black trace) and $(His)_6$-SufBC (red trace) upon initial anaerobic purification. These proteins were coexpressed with SufS and SufE, but SufD was not present in either expression vector.

The $(His)_6$-$SufBC_2D$-SufC(K40R) complex also eluted as two peaks just as observed with wild-type SufBCD (Supporting Information Figure S1B). SufC(K40R) and SufD copurified with $(His)_6$-SufB in peak 1 during the anaerobic purification in an apparent $SufBC_2D$ complex as observed for wild-type SufBCD, confirming that the SufC(K40R) mutation does not disrupt complex stoichiometry (Figure 5). Upon initial purification the UV−visible spectrum of $(His)_6$-$SufBC_2D$-SufC(K40R) peak 1 looks nearly identical to that of wild-type $(His)_6$-$SufBC_2D$ peak 1 with a broad shoulder at 320 nm and maxima at 439 nm and a lower maxima at 600 nm (Figure 6A). After 10 min air exposure, the UV−visible absorption spectrum of $(His)_6$-$SufBC_2D$-SufC(K40R) peak 1 (Figure 6A) showed maxima at 375 and 448 nm that were nearly identical to that of the wild-type $(His)_6$-$SufBC_2D$ peak 1 exposed to air for 10 min (Figure 2A). Both spectra are consistent with the oxidation of $FADH_2$ to FAD. The $(His)_6$-$SufBC_2D$-SufC(K40R) peak 1 contained 1 $FADH_2$ per complex. After anaerobic concentration, $(His)_6$-$SufBC_2D$-SufC(K40R) peak 1 still contained 0.8 $FADH_2$ per complex (Table 1). $(His)_6$-$SufBC_2D$-SufC(K40R) peak 1 only contained 0.2 Fe atom per complex, an 8-fold reduction in iron content relative to the wild-type $(His)_6$-$SufBC_2D$ peak 1 (Table 1). However, the sulfide content of $(His)_6$-$SufBC_2D$-SufC(K40R) peak 1 (1.3 S^{2-} atoms per complex) was only reduced 40% relative to the wild-type $(His)_6$-$SufBC_2D$ peak 1 (Table 1). The reduction in iron and sulfide parallels that observed for SufB or the $SufB_2C_2$ subcomplex, indicating that disruption of SufC ATPase activity impairs Fe-S cluster assembly on SufB to an equal extent as the absence of SufD or the absence of both SufC and SufD (Table 1). It appears that disruption of Fe-S cluster

assembly in the mutant complex is specifically linked to disrupted iron acquisition rather than perturbed sulfur transfer (Table 1). To independently confirm that the loss of cluster content in the $(His)_6$-$SufBC_2D$-SufC(K40R) mutant complex is not attributable to disrupted sulfur transfer, we tested if $SufBC_2D$-SufC(K40R) can still enhance the cysteine desulfurase activity of SufS in the presence of SufE. Since the mutant complex enhances SufSE activity equally as well as the wild-type $SufBC_2D$ complex (Table 2), the SufC-(K40R) mutation likely does not directly perturb sulfur transfer.

SDS−PAGE analysis of peak 2 revealed that levels of SufC and SufD protein were reduced compared to peak 1 just as was observed for wild-type $(His)_6$-$SufB_2C_2$ peak 2 (Figure 5 and Supporting Information Table S1). The UV−visible absorption spectra of $(His)_6$-$SufB_2C_2$-SufC(K40R) peak 2 showed weak Fe-S cluster features with a broad but low intensity maxima at 413 nm (Figure 6B). After anaerobic concentration, $(His)_6$-$SufB_2C_2$-SufC(K40R) peak 2 had an 8-fold reduction in iron content (0.4 Fe atom per complex) compared to the wild-type $(His)_6$-$SufB_2C_2$ peak 2 (Table 1). However, the sulfide content of $(His)_6$-$SufB_2C_2$-SufC(K40R) peak 2 was only reduced 3.7-fold compared to wild-type $(His)_6$-$SufB_2C_2$ peak 2 (1.1 S^{2-} atoms per complex). In contrast to wild-type $(His)_6$-$SufB_2C_2$ peak 2, $(His)_6$-$SufB_2C_2$-SufC(K40R) peak 2 contained only trace amounts of $FADH_2$ (0.1 per complex). These results indicate that the SufC ATPase activity is required for in vivo Fe-S cluster formation on SufB. Loss of SufC ATPase activity leads to a significant decrease in the iron content of $(His)_6$-$SufBC_2D$ peak 1 and $(His)_6$-$SufB_2C_2$ peak 2 with a less severe reduction of sulfide content.

To directly test if SufC ATPase activity is required for in vivo Suf function, SufC Lys40 was mutated to Arg in the pGSO164 plasmid, which contains the entire *sufABCDSE* operon under the control of an arabinose-inducible promoter. We determined if the SufC(K40R) mutant plasmid could rescue the growth defect of the Δ*sufABCDSE* strain under iron starvation conditions using the ferrous iron chelator 2,2′-dipyridyl (Figure 7). The wild-type pGSO164 plasmid was able to fully rescue the Δ*sufABCDSE* strain under iron starvation conditions (Figure 7). In contrast, the SufC(K40R) mutation completely abolished the ability of the pGSO164 to rescue the Δ*sufABCDSE* strain, confirming that SufC ATPase activity is absolutely required for Fe-S cluster biosynthesis during iron starvation stress in *E. coli* (Figure 7).

The SufBCDSE Cluster Assembly Pathway Can Be Activated in Cell Lysates by the Addition of ATP and NADPH. The $SufB_2C_2$ complex isolated after coexpression with SufD (peak 2) contains 3.2 Fe per complex, consistent with 0.40 [4Fe-4S] clusters bound to each SufB monomer in the complex. The isolated $SufBC_2D$ complex contains 1.3 Fe per complex, which equates to 0.33 [4Fe-4S] cluster per SufB monomer in the complex. If we assume that SufB in both complexes may bind a [4Fe-4S] cluster in vivo as has been shown in vitro (*7*, *13*), it appears that both complexes contain less than their full theoretical complement of [4Fe-4S] cluster. The lack of complete cluster binding by SufB suggests that one or more substrates required for cluster assembly are limiting in our in vivo expression system.

The three confirmed substrates required by Suf are L-cysteine for SufSE sulfur donation, ATP for SufC ATPase activity, and an iron source. Therefore, we attempted to reactivate the Suf assembly pathway in cell lysates from cells coexpressing SufBCD and SufSE by adding exogenous L-cysteine and ATP to freshly prepared cell lysates under anaerobic conditions. Due to the potential role of $FADH_2$ in the Suf system, exogenous NADPH

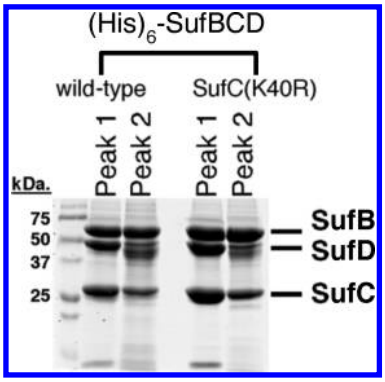

FIGURE 5: SDS−PAGE analysis of proteins and complexes purified using $(His)_6$-SufB expressed from pFWO470 and pFWO471 (containing the SufC K40R mutation). Samples from each anaerobic purification were separated on a 12% SDS−PAGE gel and stained with Coomassie blue stain.

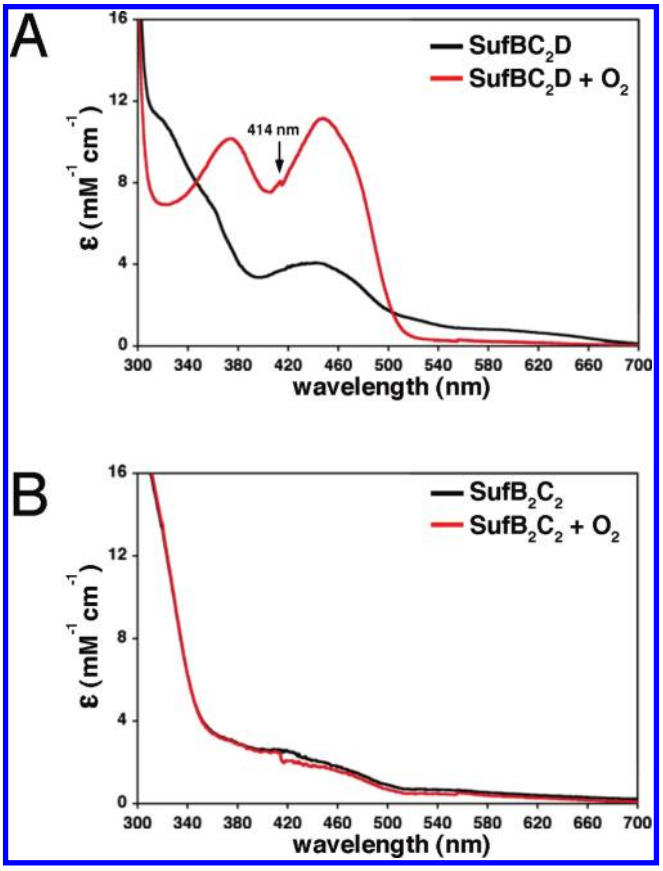

FIGURE 6: UV−visible absorption spectra of anaerobically purified $(His)_6$-$SufBC_2D$ peak 1 (A) and $(His)_6$-$SufB_2C_2$ peak 2 (B) complexes containing the SufC(K40R) point mutation. Black traces are spectra taken upon initial anaerobic purification, and red traces are spectra of the same samples taken after subsequent 10 min exposure to air. Note that SufS and SufE also were coexpressed with SufBCD in these experiments.

was also added to serve as source of reducing equivalents for redox cycling of $FAD/FADH_2$. Since the in vivo iron donor is unknown, no exogenous iron source was added. Only endogenous iron donors/sources already present in the cell lysate could be used for cluster assembly. After incubating the lysates with various combinations of L-cysteine, ATP, and/or NADPH for 120 min, $(His)_6$-SufB was purified under anaerobic conditions as described for the other purifications above. Two distinct complexes ($SufBC_2D$ and $SufB_2C_2$) were isolated during the

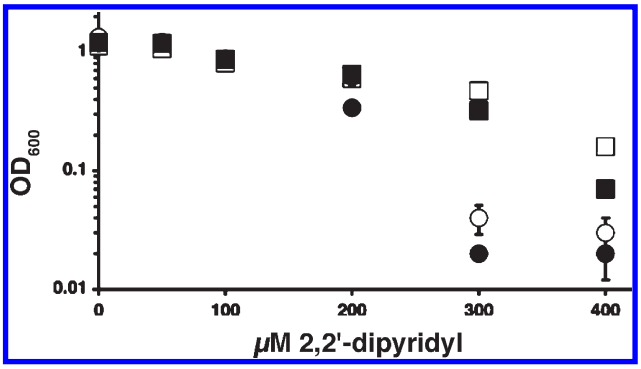

FIGURE 7: Complementation of the Δ*sufABCDSE* mutation in trans with pGSO164 and pGSO164 SufC(K40R) plasmids. The following *E. coli* strains were diluted to the same starting cell density into M9/gluconate media containing increasing amounts of 2,2′-dipyridyl: wild type (open squares), Δ*sufABCDSE* (open circles), Δ*sufABCDSE* pGSO164 (filled squares), and Δ*sufABCDSE* pGSO164-SufC(K40R) (closed circles). Final growth was measured as OD_{600} after 14 h at 37 °C. The arabinose-regulated promoter in pGSO164 has significant basal expression, and arabinose addition was not required for complementation.

purification, and the approximate ratios of protein in both complexes did not significantly change (data not shown).

After incubation with only exogenous L-cysteine in the lysate, the UV−visible absorption spectrum of purified $SufBC_2D$ (Figure 8A) showed a spectrum similar to $SufBC_2D$ purified without incubation with L-cysteine (Figure 2A). After incubation with L-cysteine + NADPH, there was a slight increase in the overall intensity of the broad 430 nm peak (Figure 8A). After incubation with L-cysteine + ATP, the $SufBC_2D$ spectrum showed a further increase in the 430 nm peak, an increase in the 320 nm shoulder, and a broad peak appearing at 620 nm (Figure 8A). After incubation with L-cysteine + ATP + NADPH, the $SufBC_2D$ spectrum looked quite similar to that obtained with just L-cysteine + NADPH, except for a slight increase in the 320 nm shoulder feature.

The UV−visible absorption spectrum of the purified $SufB_2C_2$ complex after incubation with L-cysteine in the lysate (Figure 8B) looked similar to $SufB_2C_2$ purified without incubation with L-cysteine (Figure 2B), including the broad peak at 420 nm. After incubation with L-cysteine + ATP, the $SufB_2C_2$ spectrum increased substantially in intensity (Figure 8B). The 420 nm peak doubled in intensity and showed a slight sharpening. Incubation with L-cysteine + ATP also resulted in the appearance of new features in the $SufB_2C_2$ spectrum at approximately 520 and 615 nm (Figure 8B). After incubation with L-cysteine + ATP + NADPH, the $SufB_2C_2$ spectrum further increased in intensity such that the 420 nm absorption was nearly triple that observed after addition of L-cysteine alone. The 420 nm peak also continued to sharpen in contrast to the broader 420 nm peak observed after addition of L-cysteine alone. The 520 nm feature was still present in the spectrum while the 620 nm absorption feature shifted slightly to approximately 600 nm. The dramatic changes in the UV−visible absorption spectra of $SufB_2C_2$ suggest that ATP is able to reactivate cluster assembly in the cell lysate resulting in an increase in the Fe-S cluster content of $SufB_2C_2$. Addition of ATP + NADPH further increases cluster assembly on $SufB_2C_2$ although NADPH alone causes only a modest change in the spectrum (Figure 8B).

Chemical analysis of $SufBC_2D$ and $SufB_2C_2$ purified from the various lysates closely agreed with the trends observed in the

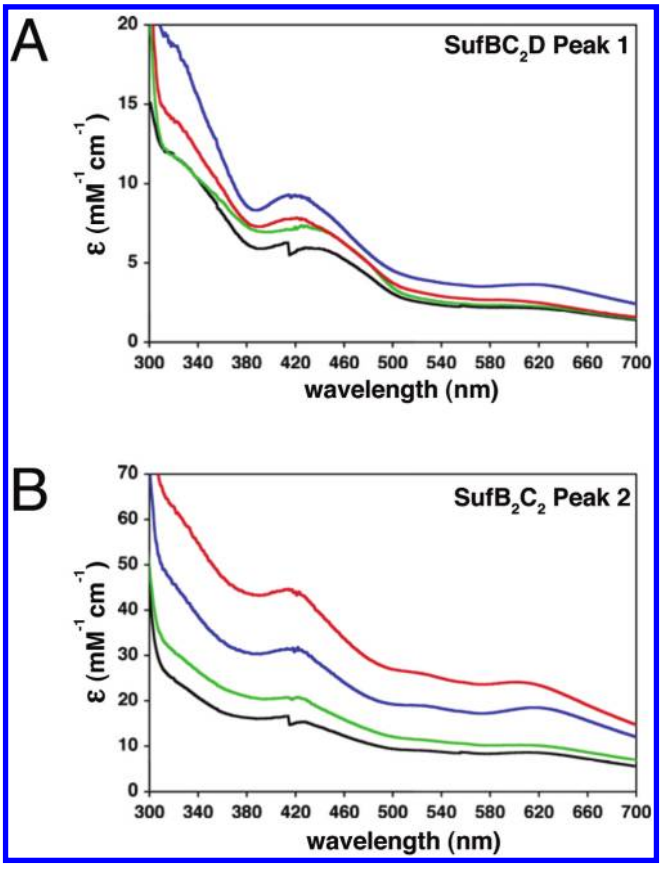

FIGURE 8: UV−visible absorption spectra of anaerobically purified $(His)_6$-$SufBC_2D$ peak 1 (A) and $(His)_6$-$SufB_2C_2$ peak 2 (B) complexes. Suf complexes were purified after 120 min incubation in crude cell lysates containing 2 mM each of L-cysteine (black trace), L-cysteine + NADPH (green trace), L-cysteine + ATP (blue trace), or L-cysteine + ATP + NADPH (red trace). Note that SufS and SufE also were coexpressed with SufBCD in the crude cell lysates used for these experiments.

UV−visible absorption spectra. Addition of L-cysteine, ATP, and/or NADPH had little net effect on the iron, acid-labile sulfide, or FAD content of $SufBC_2D$ (Table 3). In contrast, addition of L-cysteine + ATP increased the iron content of $SufB_2C_2$ from ≈3.0 Fe atoms per complex to 6.4 Fe atoms per $SufB_2C_2$ (Table 3). The acid-labile sulfide content of $SufB_2C_2$ similarly increased from 3.3 S^{2-} per complex to 6.8 S^{2-} per complex. Addition of L-cysteine + ATP + NADPH further increased iron content to 7.6 Fe per $SufB_2C_2$ and sulfide content to 7.8 S^{2-} per $SufB_2C_2$. FAD content of $SufB_2C_2$ was not significantly altered by the various additions (Table 3). The UV−visible absorption spectra and chemical analysis show that addition of L-cysteine + ATP + NADPH to the cell lysate was able to reactivate the Suf system leading to an approximate doubling of cluster content on $SufB_2C_2$ such that each SufB subunit contains sufficient iron and sulfide to form a [3Fe-4S] or [4Fe-4S] cluster. There was no significant net change in $SufBC_2D$ iron and sulfur content in response to the same treatment, although it is worth noting that transient changes in $SufBC_2D$ may not be apparent in these end point measurements (after 120 min incubation) and might occur at intermediate time points in the experiment.

Since Fe-S cluster accumulates in $SufB_2C_2$ when the system is reactivated in a cell lysate, this result provides additional support for the model that $SufB_2C_2$ is the mature cluster-containing complex. This result also indicates that ATP + NADPH is sufficient to reactivate iron acquisition using endogenous iron

sources found in the cell lysate and is consistent with the selective depletion of iron content in the SufC_K40R mutant complexes which lack ATPase activity. The results suggest that ATP and/or a source of reducing equivalents (NADPH) may be somewhat limiting in our in vivo expression experiments, thereby limiting the total level of in vivo Fe-S cluster assembly on the Suf proteins.

DISCUSSION

SufC and SufD Are Critical for in Vivo Fe-S Cluster Biosynthesis. Our results clearly demonstrate the importance of SufC and SufD for in vivo Fe-S cluster assembly on SufB. Despite the relative ease of reconstituting [4Fe-4S] SufB in vitro (*7*), disruption of SufC or SufD by deletion or point mutation abolishes most in vivo cluster assembly on SufB (Figures 4 and 6, Table 1). These studies also establish that at least two distinct complexes can exist in vivo, $SufBC_2D$ (peak 1) and $SufB_2C_2$ (peak 2). The $SufB_2C_2$ complex was purified previously after coexpressing SufB and SufC-$(His)_6$, but this subcomplex was not analyzed for cluster content or flavin binding (*16*). Surprisingly, if SufB and SufC are purified separately and then mixed in vitro, a novel complex with $SufBC_2$ stoichiometry is generated (*13*), suggesting there is a posttranscriptional mechanism to ensure proper complex formation in vivo.

On the basis of spectroscopic and chemical analysis, we isolated $SufBC_2D$ that contains $FADH_2$ and a substoichiometric amount of Fe-S cluster species (peak 1) and $SufB_2C_2$ that lacks most SufD and has lower levels of $FADH_2$ but contains a [4Fe-4S] cluster (peak 2). The increased iron and sulfide present in $SufB_2C_2$ peak 2 logically place this conformational intermediate downstream of the $SufBC_2D$ conformation in peak 1. These results indicate that SufD is required for in vivo iron acquisition to complete the Fe-S cluster in the SufBC subcomplex, but during cluster assembly or upon cluster maturation, SufCD dissociates from SufBC, possibly allowing the formation of $SufB_2C_2$ (Scheme 1). This hypothesis is supported by our results showing that the $SufB_2C_2$ subcomplex (expressed in the absence of SufD) cannot mature to the [4Fe-4S] form in vivo, largely because

Table 3: Chemical Analysis of Purified Complex after Suf Reactivation in Cell Lysates

		addition			
complex purified[a]		L-Cys	L-Cys + NADPH	L-Cys + ATP	L-Cys + ATP + NADPH
$SufBC_2D$ peak 1	Fe:complex[b]	1.7 ± 0.01	1.4 ± 0.3	1.8 ± 0.07	1.2 ± 0.03
	S^{2-}:complex[b]	2.1 ± 0.8	2.2 ± 0.2	2.3 ± 0.6	2.4 ± 0.9
	FAD:complex[b]	1.0 ± 0.1	1.0 ± 0.02	1.3 ± 0.02	1.1 ± 0.4
$SufB_2C_2$ peak 2	Fe:complex[b]	3.0 ± 0.07	3.1 ± 0.5	6.4 ± 0.04	7.6 ± 0.17
	S^{2-}:complex[b]	3.3 ± 0.4	3.4 ± 0.9	6.8 ± 0.7	7.8 ± 1.0
	FAD:complex[b]	0.4 ± 0.04	0.5 ± 0.3	0.4 ± 0.05	0.6 ± 0.3

[a]All proteins were purified from cells also coexpressing SufS and SufE (see text for details). See Materials and Methods for molecular masses used to determine ratios of protein to iron and sulfide. [b]Average of triplicate measurements of samples.

Scheme 1: Model for in Vivo Suf Fe-S Cluster Assembly[a]

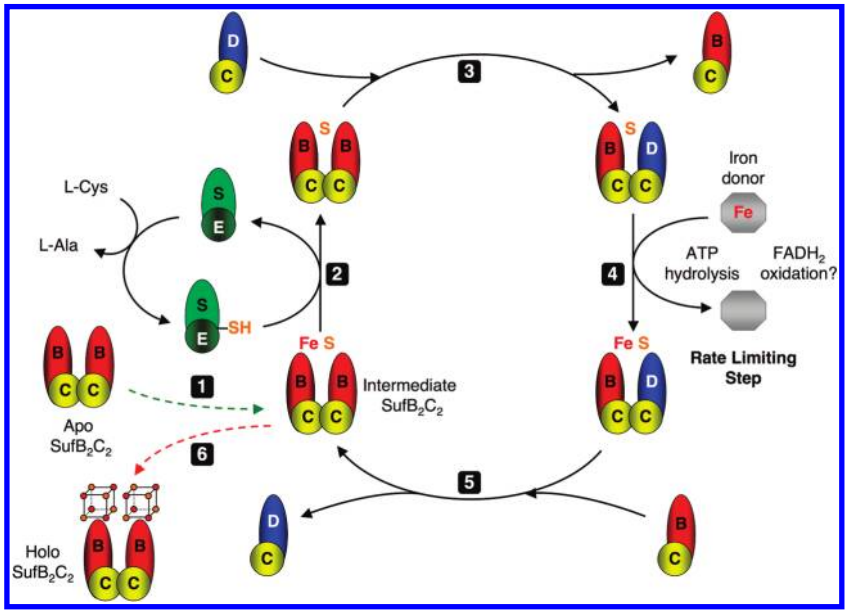

[a]Sulfur is mobilized from L-cysteine by SufSE and transferred to apo $SufB_2C_2$ (steps 1 and 2). SufBC interacts with SufCD in the $SufBC_2D$ complex for iron acquisition, ATP hydrolysis, and possibly $FADH_2$ oxidation (steps 3 and 4). A $SufB_2C_2$ intermediate containing substoichiometric iron and sulfide begins another cycle (step 5). After multiple cycles, $SufB_2C_2$ forms 2 × [4Fe-4S] clusters and exits the cycle for cluster transfer (step 6). The exact mechanism of SufD/SufB association and dissociation during the reaction cycle is unknown, but we show the cycle proceeding through exchange of $SufB_1C_1$ and $SufC_1D_1$ heterodimer intermediates. A second interlocking cycle could be occurring simultaneously with exchange of $SufB_1C_1$ and $SufC_1D_1$ intermediates connecting the two cycles (not shown for simplicity). The green arrow shows entry of apo $SufB_2C_2$ into the cycle. The red arrow indicates maturation of $SufB_2C_2$ into the 2 × [4Fe-4S] form.

in vivo iron acquisition is blocked (Table 1 and Figure 4). This result also argues against a postassembly role for SufD in Fe-S cluster transfer. If SufD is utilized for Fe-S cluster transfer, one would predict that the cluster content of $SufB_2C_2$ would remain unchanged or perhaps increase in the absence of SufD due to lack of Fe-S cluster transfer to target enzymes. Instead, we obtained the opposite result showing that lack of SufD blocks de novo Fe-S cluster formation in $SufB_2C_2$.

The reproducible copurification of SufS with $SufB_2C_2$ (Figure 1 and Supporting Information Figure S2B) suggests that in vivo sulfur donation actually occurs between SufSE and $SufB_2C_2$. This hypothesis is supported by previous studies showing that SufBC is the minimum complex necessary for SufB to interact with SufE and for stimulation of SufSE cysteine desulfurase activity while SufD is not required (*7*). All current in vitro and in vivo data indicate that SufD and ATP hydrolysis by SufC are not utilized during sulfur transfer to SufB (*9*, *29*). Scheme 1 shows one model consistent with these data where the Suf scaffold system cycles between $SufB_2C_2$-SufSE (for sulfur acquisition) and $SufBC_2D$ (for iron acquisition) until the mature 2[4Fe-4S] $SufB_2C_2$ complex is achieved. Since sulfide donation appears to still occur despite a block in iron acquisition (caused by loss of SufC ATPase activity or loss of SufD), this supports the "sulfur first" model of stepwise Fe-S cluster assembly (*30*, *31*). The purification results show that $<80\%$ of the SufBCD scaffold system is in the $SufBC_2D$ conformation under steady-state expression conditions, suggesting that iron acquisition by $SufBC_2D$ is the rate-limiting step of cluster assembly in vivo. While this model awaits further testing at the biochemical level, it is consistent with phylogenetic analysis showing that only SufB and SufC strictly co-occur among Archael and Eubacterial genomes while SufD is sometimes lacking (*6*). The $SufB_2C_2$ complex may therefore constitute the core scaffold complex while SufD is an adaptor protein used for iron acquisition in specific organisms or under specific environmental conditions.

It was previously shown that cluster assembly on the IscU scaffold protein proceeds via reductive coupling of two [2Fe-2S] clusters to generate a [4Fe-4S] cluster (*25*). Interestingly, we did not observe stable [2Fe-2S] intermediate forms of SufBCD during our purification. Instead, we obtained preliminary evidence for the presence of a linear [3Fe-4S] cluster bound to SufBCD. At present we cannot definitively assign the linear [3Fe-4S] cluster to either $SufBC_2D$ or $SufB_2C_2$. We also cannot determine if the linear [3Fe-4S] cluster is a degradation product derived from a cuboidal [4Fe-4S] cluster or a bona fide intermediate during Fe-S cluster assembly. If the linear [3Fe-4S] cluster is a stable intermediate formed during assembly of the [4Fe-4S] cluster on $SufB_2C_2$, this would indicate that the Suf pathway uses a novel cluster assembly mechanism compared to the well-characterized Isc system.

SufC ATPase Activity and SufD May Work Together for in Vivo Iron Acquisition. The iron content of all SufBCD complexes is reduced if SufC lysine 40 is mutated to arginine. Furthermore, addition of ATP to cell lysates expressing the wild-type SufBCDSE proteins can reactivate the Suf system leading to a doubling of the Fe-S cluster content of $SufB_2C_2$ (Figure 8, Table 3). These results indicate that SufC ATP hydrolysis is likely used for iron acquisition during in vivo Fe-S cluster assembly by the Suf pathway. Since the absence of SufD diminishes the iron content of the $SufB_2C_2$ subcomplex to a similar extent as the SufC K40R mutation reduces iron content in $SufBC_2D$ peak 1 and $SufB_2C_2$ peak 2 (Table 1), we propose that SufC ATPase activity works in concert with SufD to provide iron for in vivo Fe-S cluster assembly by the Suf pathway.

The need to expend energy for iron acquisition (in the form of ATP hydrolysis) is logical as the Suf pathway functions under iron starvation conditions where bioavailable iron is limiting. Similarly, during hydrogen peroxide stress most of the labile iron pool available for cofactor biosynthesis is sequestered in iron storage proteins, especially the dodecameric ferritin homologue Dps, in order to minimize Fenton chemistry (*32*). Therefore, Suf must accumulate bioavailable iron against a considerable concentration gradient created by iron sequestration into storage proteins in order to carry out in vivo Fe-S cluster assembly. In contrast to the defects in iron acquisition, the SufC K40R mutation or omission of SufD reduced in vivo sulfur donation to SufB to a much less extent (Table 1). The partial reduction in sulfide content could result from aborted cluster assembly due to reduced iron acquisition or from subtle structural changes in the $SufB_2C_2$ subcomplex or $SufBC_2D$ complex. Our current results suggest that ATP hydrolysis helps to drive in vivo iron acquisition by $SufBC_2D$ but they do not rule out additional roles for SufC in cluster transfer or binding to target apoproteins. Further experiments are necessary to delineate the functional differences between $SufBC_2D$ and $SufB_2C_2$, and SufC ATPase activity may very well have differential roles in each complex.

As noted above, the isolation of $FADH_2$ $SufBC_2D$ using our expression system parallels other recent studies (*13*). In addition, we show here that the $SufBC_2D$-SufC(K40R) peak 1 complex (which is blocked for ATP hydrolysis) can still bind 1 equiv of $FADH_2$ just as wild-type $SufBC_2D$. In contrast, the flavin content of the $SufB_2C_2$-SufC(K40R) peak 2 complex decreased from 0.4 to 0.1 per complex (Table 1). Currently, it is not clear if $FADH_2$ is actually required for in vivo Fe-S cluster assembly by the Suf pathway. Reducing equivalents donated by $FADH_2$ may be used in vivo for iron acquisition, especially to reduce Fe^{3+} to Fe^{2+} to release it from iron storage proteins or siderophores. Wollers et al. demonstrated that $FADH_2$ $SufBC_2D$ can reduce Fe^{3+} to Fe^{2+} in small chelates (ferric citrate) and ferric iron binding proteins (CyaY), although free flavin was more efficient than $FADH_2$ $SufBC_2D$ for reducing ferric citrate (*13*). Alternatively, $FADH_2$ may help to reduce persulfide (S^0) to generate a bridging sulfide (S^{2-}) or could drive reductive coupling of [2Fe-2S] clusters during cluster assembly. Future studies are necessary to clarify the role of $FADH_2$ (if any) in the Suf pathway.

In summary, we present both in vitro and in vivo evidence that the SufBCD scaffold system can form [3Fe-4S] and [4Fe-4S] clusters in vivo and that SufC ATPase activity and SufD are required for iron acquisition during in vivo Fe-S cluster assembly. Our results also suggest that distinct subcomplexes form among the SufB, SufC, and SufD proteins during cluster assembly in vivo and that the mature [4Fe-4S] cluster is bound to the $SufB_2C_2$ complex.

ACKNOWLEDGMENT

We thank Dr. C. E. Outten and Dr. R. Drevland for helpful comments on the manuscript.

SUPPORTING INFORMATION AVAILABLE

Supplemental methods for protein stoichiometry measurements and in vitro Fe-S cluster reconstitution of SufBCD, Table S1 containing the stoichiometry measurements for the various complexes, Figure S1 containing the elution profile of wild-type and SufC(K40R) $(His)_6$-SufBCD, Figure S2 containing

the UV−visible absorption spectrum of the flow-through after SufBCD concentration and the identification of low intensity bands in the $(His)_6$-SufBCD elution fractions, and Figure S3 containing the EPR spectrum of in vitro reconstituted $[4Fe\text{-}4S]^+$ SufBCD. This material is available free of charge via the Internet at http://pubs.acs.org.

REFERENCES

1. Lill, R. (2009) Function and biogenesis of iron-sulphur proteins. *Nature 460*, 831–838.
2. Ayala-Castro, C., Saini, A., and Outten, F. W. (2008) Fe-S cluster assembly pathways in bacteria. *Microbiol. Mol. Biol. Rev. 72*, 110–125.
3. Nachin, L., El Hassouni, M., Loiseau, L., Expert, D., and Barras, F. (2001) SoxR-dependent response to oxidative stress and virulence of *Erwinia chrysanthemi*: the key role of SufC, an orphan ABC ATPase. *Mol. Microbiol. 39*, 960–972.
4. Nachin, L., Loiseau, L., Expert, D., and Barras, F. (2003) SufC: an unorthodox cytoplasmic ABC/ATPase required for [Fe-S] biogenesis under oxidative stress. *EMBO J. 22*, 427–437.
5. Outten, F. W., Djaman, O., and Storz, G. (2004) A *suf* operon requirement for Fe-S cluster assembly during iron starvation in *Escherichia coli*. *Mol. Microbiol. 52*, 861–872.
6. Takahashi, Y., and Tokumoto, U. (2002) A third bacterial system for the assembly of iron-sulfur clusters with homologs in archaea and plastids. *J. Biol. Chem. 277*, 28380–28383.
7. Layer, G., Gaddam, S. A., Ayala-Castro, C. N., Ollagnier-de Choudens, S., Lascoux, D., Fontecave, M., and Outten, F. W. (2007) SufE transfers sulfur from SufS to SufB for iron-sulfur cluster assembly. *J. Biol. Chem. 282*, 13342–13350.
8. Loiseau, L., Ollagnier-de-Choudens, S., Nachin, L., Fontecave, M., and Barras, F. (2003) Biogenesis of Fe-S cluster by the bacterial Suf system: SufS and SufE form a new type of cysteine desulfurase. *J. Biol. Chem. 278*, 38352–38359.
9. Outten, F. W., Wood, M. J., Munoz, F. M., and Storz, G. (2003) The SufE protein and the SufBCD complex enhance SufS cysteine desulfurase activity as part of a sulfur transfer pathway for Fe-S cluster assembly in *Escherichia coli*. *J. Biol. Chem. 278*, 45713–45719.
10. Gupta, V., Sendra, M., Naik, S. G., Chahal, H. K., Huynh, B. H., Outten, F. W., Fontecave, M., and Ollagnier de Choudens, S. (2009) Native *Escherichia coli* SufA, co-expressed with SufBCDSE, purifies as a [2Fe-2S] protein and acts as an Fe-S transporter to Fe-S target enzymes. *J. Am. Chem. Soc. 131*, 6149–6153.
11. Ollagnier-de-Choudens, S., Sanakis, Y., and Fontecave, M. (2004) SufA/IscA: reactivity studies of a class of scaffold proteins involved in [Fe-S] cluster assembly. *J. Biol. Inorg. Chem. 9*, 828–838.
12. Vinella, D., Brochier-Armanet, C., Loiseau, L., Talla, E., and Barras, F. (2009) Iron-sulfur (Fe/S) protein biogenesis: phylogenomic and genetic studies of A-type carriers. *PLoS Genet. 5*, e1000497.
13. Wollers, S., Layer, G., Garcia-Serres, R., Signor, L., Clemancey, M., Latour, J. M., Fontecave, M., and Ollagnier de Choudens, S. (2010) Iron-sulfur (Fe-S) cluster assembly: the SufBCD complex is a new type of Fe-S scaffold with a flavin redox cofactor. *J. Biol. Chem. 285*, 23331–23341.
14. Chahal, H. K., Dai, Y., Saini, A., Ayala-Castro, C., and Outten, F. W. (2009) The SufBCD Fe-S scaffold complex interacts with SufA for Fe-S cluster transfer. *Biochemistry 48*, 10644–10653.
15. Eccleston, J. F., Petrovic, A., Davis, C. T., Rangachari, K., and Wilson, R. J. (2006) The kinetic mechanism of the SufC ATPase: the cleavage step is accelerated by SufB. *J. Biol. Chem. 281*, 8371–8378.
16. Petrovic, A., Davis, C. T., Rangachari, K., Clough, B., Wilson, R. J., and Eccleston, J. F. (2008) Hydrodynamic characterization of the SufBC and SufCD complexes and their interaction with fluorescent adenosine nucleotides. *Protein Sci. 17*, 1264–1274.
17. Riemer, J., Hoepken, H. H., Czerwinska, H., Robinson, S. R., and Dringen, R. (2004) Colorimetric ferrozine-based assay for the quantitation of iron in cultured cells. *Anal. Biochem. 331*, 370–375.
18. Beinert, H. (1983) Semi-micro methods for analysis of labile sulfide and of labile sulfide plus sulfane sulfur in unusually stable iron-sulfur proteins. *Anal. Biochem. 131*, 373–378.
19. Coves, J., Zeghouf, M., Macherel, D., Guigliarelli, B., Asso, M., and Fontecave, M. (1997) Flavin mononucleotide-binding domain of the flavoprotein component of the sulfite reductase from *Escherichia coli*. *Biochemistry 36*, 5921–5928.
20. Koziol, J. (1971) Fluorometric analyses of riboflavin and its coenzyme, in Methods in Enzymology (McCormick, D. B., and Wright, L. D., Eds.) pp 253−285, Academic, New York.
21. Lee, J. H., Yeo, W. S., and Roe, J. H. (2004) Induction of the *sufA* operon encoding Fe-S assembly proteins by superoxide generators and hydrogen peroxide: involvement of OxyR, IHF and an unidentified oxidant-responsive factor. *Mol. Microbiol. 51*, 1745–1755.
22. Tokumoto, U., Kitamura, S., Fukuyama, K., and Takahashi, Y. (2004) Interchangeability and distinct properties of bacterial Fe-S cluster assembly systems: functional replacement of the *isc* and *suf* operons in *Escherichia coli* with the nifSU-like operon from *Helicobacter pylori*. *J. Biochem. 136*, 199–209.
23. Kennedy, M. C., Kent, T. A., Emptage, M., Merkle, H., Beinert, H., and Munck, E. (1984) Evidence for the formation of a linear [3Fe-4S] cluster in partially unfolded aconitase. *J. Biol. Chem. 259*, 14463–14471.
24. Richards, A. J. M., Thomson, A. J., Holm, R. H., and Hagen, K. S. (1990) The magnetic circular dichroism spectra of the linear trinuclear clusters $[Fe_3S_4(SR)_4]^{3-}$ in purple aconitase and in a synthetic model. *Spectrochim. Acta 46A*, 987–993.
25. Chandramouli, K., Unciuleac, M. C., Naik, S., Dean, D. R., Huynh, B. H., and Johnson, M. K. (2007) Formation and properties of [4Fe-4S] clusters on the IscU scaffold protein. *Biochemistry 46*, 6804–6811.
26. Hagen, K. S., Watson, A. D., and Holm, R. H. (1983) Synthetic routes to Fe_2S_2, Fe_3S_4, Fe_4S_4, and Fe_6S_9 clusters from the common precursor $[Fe(SC_2H_5)_4]^{2-}$. Structures and properties of $[Fe_3S_4(SR)_4]^{3-}$ and $[Fe_6S_9(SC_2H_5)_2]^{4-}$, examples of the newest types of Fe-S-SR clusters. *J. Am. Chem. Soc. 105*, 3905–3913.
27. Wada, K., Sumi, N., Nagai, R., Iwasaki, K., Sato, T., Suzuki, K., Hasegawa, Y., Kitaoka, S., Minami, Y., Outten, F. W., Takahashi, Y., and Fukuyama, K. (2009) Molecular dynamism of Fe-S cluster biosynthesis implicated by the structure of $SufC_2$-$SufD_2$ complex. *J. Mol. Biol. 387*, 245–258.
28. Schneider, E., Wilken, S., and Schmid, R. (1994) Nucleotide-induced conformational changes of MalK, a bacterial ATP binding cassette transporter protein. *J. Biol. Chem. 269*, 20456–20461.
29. Layer, G., Ollagnier de Choudens, S., Sanakis, Y., and Fontecave, M. (2006) Iron-sulfur cluster biosynthesis: characterization of *Escherichia coli* CyaY as an iron donor for the assembly of [2Fe-2S] clusters in the scaffold IscU. *J. Biol. Chem. 281*, 16256–16263.
30. Fontecave, M., Choudens, S. O., Py, B., and Barras, F. (2005) Mechanisms of iron-sulfur cluster assembly: the SUF machinery. *J. Biol. Inorg. Chem. 10*, 713–721.
31. Krebs, C., Agar, J. N., Smith, A. D., Frazzon, J., Dean, D. R., Huynh, B. H., and Johnson, M. K. (2001) IscA, an alternate scaffold for Fe-S cluster biosynthesis. *Biochemistry 40*, 14069–14080.
32. Park, S., You, X., and Imlay, J. A. (2005) Substantial DNA damage from submicromolar intracellular hydrogen peroxide detected in Hpx- mutants of *Escherichia coli*. *Proc. Natl. Acad. Sci. U.S.A. 102*, 9317–9322.